

Surge of neurophysiological coherence and connectivity in the dying brain

Jimo Borjigin^{a,b,c,1,2}, UnCheol Lee^{d,1}, Tiecheng Liu^a, Dinesh Pal^d, Sean Huff^a, Daniel Klarr^d, Jennifer Sloboda^a, Jason Hernandez^a, Michael M. Wang^{a,b,c,e}, and George A. Mashour^{c,d}

Departments of ^aMolecular and Integrative Physiology, ^bNeurology, and ^dAnesthesiology, and ^cNeuroscience Graduate Program, University of Michigan, Ann Arbor, MI 48109; and ^eVeterans Administration, Ann Arbor, MI 48105

Edited by Solomon H. Snyder, The Johns Hopkins University School of Medicine, Baltimore, MD, and approved July 9, 2013 (received for review May 2, 2013)

The brain is assumed to be hypoactive during cardiac arrest. However, the neurophysiological state of the brain immediately following cardiac arrest has not been systematically investigated. In this study, we performed continuous electroencephalography in rats undergoing experimental cardiac arrest and analyzed changes in power density, coherence, directed connectivity, and cross-frequency coupling. We identified a transient surge of synchronous gamma oscillations that occurred within the first 30 s after cardiac arrest and preceded isoelectric electroencephalogram. Gamma oscillations during cardiac arrest were global and highly coherent; moreover, this frequency band exhibited a striking increase in anterior–posterior-directed connectivity and tight phase-coupling to both theta and alpha waves. High-frequency neurophysiological activity in the near-death state exceeded levels found during the conscious waking state. These data demonstrate that the mammalian brain can, albeit paradoxically, generate neural correlates of heightened conscious processing at near-death.

global ischemia | global hypoxia | near-death experience | consciousness

The human brain possesses the capacity to generate internal states of consciousness during dreaming (1), hallucinations (2, 3), and meditation (4). Internally generated visions and perceptions are also reported by ~20% of cardiac arrest survivors during clinical death (5–7). These near-death experiences (NDE) (8), reported worldwide across cultures (9), are described to be highly lucid and vivid, and are perceived to be “realer than real” (10). Whether and how the brain is capable of generating conscious activity during cardiac arrest has been vigorously debated (11–13). We reasoned that if NDE stems from brain activity, neural correlates of consciousness should be identifiable in humans or animals after cessation of cerebral blood flow. In this study, we tested this hypothesis by recording and analyzing electroencephalograms (EEG) of rats during the waking state, general anesthesia, and after cardiac arrest.

Neuronal oscillations in the gamma range (>25 Hz) have been associated with waking consciousness, altered states of consciousness during meditation, and rapid eye movement sleep (1, 4, 14–18). Conscious perception is associated not only with an increase in gamma power, but also with long-range synchronization of gamma (30–80 Hz) oscillations (19). Furthermore, current perspectives on the neural correlates of consciousness suggest that cortical and thalamocortical effective connectivity is critical for conscious processing (20, 21). For example, directional information transfer across the brain is thought to play an important role in conscious perception. In the visual modality, information transfer from primary visual cortex in the occipital lobe to the frontal areas (feedforward, or bottom-up) is subliminal, whereas feedback (frontal to posterior, or top-down) information transfer is associated with conscious perception (22). In support of this, studies have shown that frontoparietal feedback processing is selectively suppressed during general anesthesia and in the vegetative state, whereas feedforward processing is preserved (23–26). In addition to gamma waves, theta rhythms also play an important role in information processing in the brain. Theta oscillations are

important for synaptic plasticity, information coding, and working memory (27, 28). Studies have shown that the theta band increases in power during both verbal and spatial memory tasks in the mammalian cortex and is a feature of cognitive control across species (29, 30). Increased theta power has also been detected in human subjects during meditation (14, 15). Recent studies suggest that cross-frequency coupling between theta and gamma rhythms may play a functional role in long-range neuronal communication, perception, and memory tasks (31–34). These findings prompted us to examine electrical oscillations of the brain by focusing on EEG power, global EEG coherence, directional brain connectivity, and cross-frequency coupling of gamma and theta waves during waking, anesthesia, and following cardiac arrest.

Results

Cardiac Arrest Stimulates a Well-Organized Series of High-Frequency EEG Events in Rat Brain. To explore the electrophysiological state of the brain following cardiac arrest, we monitored EEG signals over the frontal, parietal, and occipital cortices bilaterally in rats during wakefulness, anesthesia, and cardiac arrest. Unprocessed EEG data from a representative rat is shown in Fig. 1. Following the onset of cardiac arrest (time 0 in all panels of Fig. 1), the EEG maintained normal amplitudes for 3 s before transitioning to a period of low-amplitude and high-frequency oscillations for up to 30 s (Fig. 1*B*). We divided this early cardiac arrest period into four sequential and distinct states that were found in nine of nine animals examined (Fig. 1*B* and *C*): cardiac arrest state 1 (CAS1), which began at the last heartbeat and terminated at the loss of oxygenated blood pulse (the dashed line in Fig. 1*B*) when EEG signals showed marked reduction in amplitude; CAS2, which terminated with a characteristic short burst of delta waves (what we term the “delta blip”); CAS3, which ended when EEG amplitude dropped below 10 μ V; and finally, CAS4, which featured EEG signals (below 10 μ V) that were indistinguishable from signals at 1,200 s after cardiac arrest (Fig. 1*C*). Each state exhibited stereotyped frequencies that were conserved across all rats examined. Unlike the anesthetized state (Fig. 1*C*, *Left*), CAS1 exhibited elevated gamma oscillations near 130 Hz in all six EEG channels. The CAS2 period, in contrast, exhibited theta oscillations mixed with high-frequency gamma oscillations across all channels. CAS3 was dominated by EEG signals in the low-gamma frequency range (35–50 Hz) that were highly synchronous and appeared to be coupled to theta oscillations across all EEG

Author contributions: J.B. and M.M.W. conceived the idea of the project; J.B. and G.A.M. designed experiments; J.B., U.L., and G.A.M. planned analysis; T.L. and D.P. performed electrode implantation; J.B., T.L., D.P., S.H., and D.K. collected data; U.L. wrote analysis programs; J.B., U.L., J.S., J.H., and G.A.M. analyzed data; and J.B., U.L., M.M.W., and G.A.M. wrote the paper.

The authors declare no conflict of interest.

This article is a PNAS Direct Submission.

¹J.B. and U.L. contributed equally to this work.

²To whom correspondence should be addressed. E-mail: borjigin@umich.edu.

This article contains supporting information online at www.pnas.org/lookup/suppl/doi:10.1073/pnas.1308285110/-DCSupplemental.

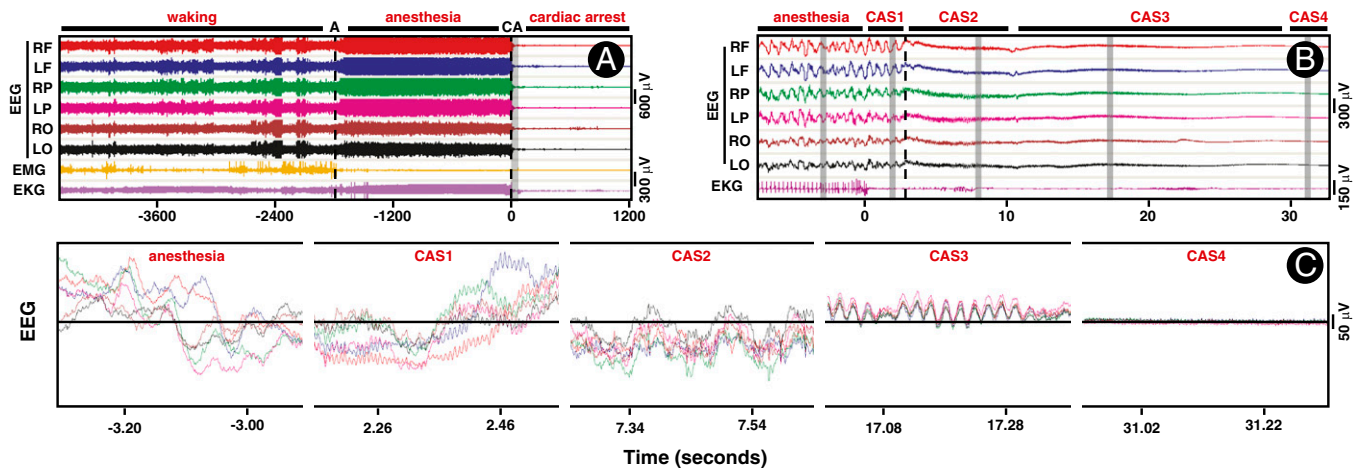


Fig. 1. EEG displays a well-organized series of high-frequency activity following cardiac arrest. (A) EEG, EMG, and EKG during 2,800 s of baseline waking state (–4585 s to –1788 s), 1,788 s of anesthetized state (–1,788 s to 0 s), and 1,216 s following cardiac arrest (0 s to 1,216 s). EEG was recorded from six regions of the rat brain: the right frontal (RF) and left frontal (LF), right parietal (RP) and left parietal (LP), and right occipital (RO) and left occipital (LO) areas. Anesthesia (A) was induced by intramuscular injection of ketamine and xylazine administered at time (T) = –1,788 s (black dashed line). Cardiac arrest (CA) was induced by intracardiac injection of potassium chloride (1 M) at T = 0 s. Both EMG and EKG signals were isoelectric within 1 s of cardiac arrest. No significant correlation of EEG with EMG and EKG signals was found in any of the frequency bands (Fig. S1). (B) The 40-s segment, shown as a vertical gray bar in A, including 8 s before and 32 s after cardiac arrest, was expanded to reveal finer features. Following the last regular cardiac discharge, EKG signals displayed several irregular bursts that were not associated with any features of the EEG. The period following cardiac arrest was divided into four distinct states: CAS1 beginning at the T = 0 s and ending at the loss of oxygenated blood pulse (LOP; marked in vertical dashed line at T = 3 s); CAS2 beginning at LOP and ending at a delta blip (a short burst of delta oscillation) at T = 11 s; CAS3 beginning at the end of the delta blip (T = 12 s) and ending when the EEG signal reached below 10 μ V at T = 30 s; and CAS4 spanning the cardiac arrest period after EEG signals were consistently below 10 μ V. (C) The selected segments in B (indicated in vertical gray bars) were further expanded, and the EEG signals from all six channels were overlaid on top of each other to reveal further details. These results are not a consequence of pain associated with the cardiac arrest procedures, as nearly identical neurophysiologic events were stimulated at near-death by CO₂ inhalation in rats (Fig. S2).

channels. CAS4 was composed of mostly 300-Hz signals that persisted for as long as recording was continued (up to 18 h). The mean durations of each of these states were 4 s (\pm 2 s) for CAS1, 6 s (\pm 1 s) for CAS2, 1.7 s (\pm 0.7 s) for delta blip, and 20 s (\pm 1 s) for CAS3. Thus, cardiac arrest induces an organized sequence of neurophysiologic events that was consistent across all rats studied. These data also suggest that this sequence includes at least two clearly defined and distinct state transitions (from CAS1 to CAS2 and from CAS2 to CAS3).

Power of Cortical Low Gamma (25–55 Hz) Oscillations Increases in the Near-Death State. Evolution of the postcardiac arrest EEG was explored first by time-frequency spectrograms (Fig. 2). Consistent with the unprocessed EEG data (Fig. 1), high-gamma waves near 130 Hz increased in power, whereas other frequency bands did not change during CAS1 (Fig. 2A, Middle). At the loss of oxygenated blood pulse, power increases were found for gamma wave clusters: a diffuse increase of low gamma (25–55 Hz) that spanned the entire CAS2 period (5 s), a short segment of medium gamma (80–100 Hz), and a residual high gamma of 130 Hz that declined early during CAS2. During this period, lower-frequency bands (<25 Hz) showed marked reduction in power, except a narrow band of theta (6–8 Hz) that persisted for the entire CAS2 period. A short burst of delta (0–5 Hz) waves separated the CAS2 and CAS3 periods and was associated with abruptly reduced beta and low-gamma (25–55 Hz) power. In contrast, the CAS3 period was distinguished by a clear increase in absolute power of low gamma (Fig. 2A, Middle) and associated with persistent theta bands. During this period, all other bands showed further decline in power. During the last 5 s of CAS3 when theta bands were still detectable, power of all other frequency bands declined further. EEG signals after the initial 30 s of cardiac arrest were indistinguishable from those recorded 20 min after the onset of cardiac arrest (Fig. 2A, Top and Middle). The CAS3 period of cardiac arrest contrasted with waking and anesthetized states in all rats. Compared with waking and

anesthetized states (Fig. 2A, Bottom), the CAS3 period was associated with dramatically reduced EEG power at all frequencies except the low-gamma (γ 1; 25–55 Hz) bands, which exhibited a significant increase ($P < 0.01$) over the waking and anesthetized periods.

These features were more prominent when the relative contribution of all frequency waves was analyzed over the entire period of recording (Fig. 2B). Following cardiac arrest, gamma waves (25–250 Hz) showed marked increase in the relative power (Fig. 2B, Top). The increase in the relative contribution of both low-gamma and the narrow-theta bands was clearly detectable following cardiac arrest, especially during the CAS3 period (Fig. 2B, Top and Middle). In fact, the low-gamma (γ 1; Fig. 2B, Bottom) bands at CAS3 showed the most dramatic increase, contributing more than 50% of the total power for all frequency bands at its peak ($P < 0.0005$). It is worth noting that low-gamma waves contributed less than 5% of the total EEG power in the waking state. Additionally, theta bands (5–10 Hz) contributed to the overall power during CAS3 at a level significantly elevated compared with the anesthetized state ($P < 0.05$), and were comparable to the waking period (Fig. 2B, Middle and Bottom).

Cardiac Arrest Stimulates a Marked Surge of Global Coherence of EEG Signals. In addition to the increase of gamma power (Figs. 1 and 2), a large increase of mean coherence for gamma oscillations was detected at near-death (Fig. 3). During the waking period, EEG signals displayed typical mean coherence among frontal, parietal, and occipital areas (Fig. 3A, Upper); high coherence levels were notable for EEG waves lower than 20 Hz and higher than 80 Hz. In contrast, during ketamine/xylazine-induced anesthesia, mean coherence was markedly reduced in all frequency bands, except for a distinct high-gamma bandwidth of 130–170 Hz (Fig. 3A, Upper). It is worth noting that the high-gamma oscillations (130–170 Hz) contributed to less than 1% of the total EEG power in the anesthetized state, and that slower waves (<15 Hz), including delta ($P < 0.05$) and theta ($P < 0.05$) bands, increased significantly

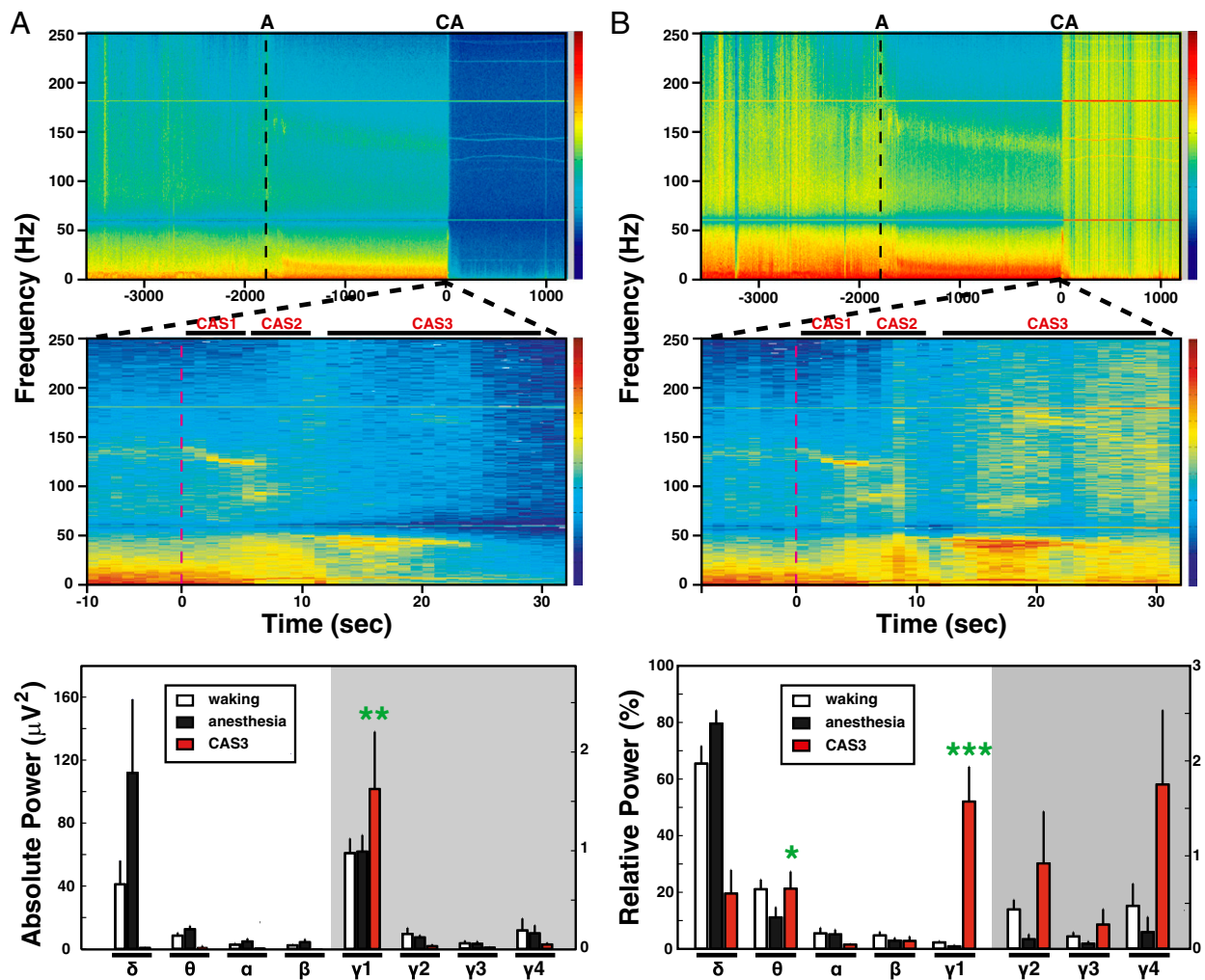


Fig. 2. Gamma power increases after cardiac arrest. (A) The spectrograms of absolute power averaged over the six EEG channels during waking (30 min), anesthesia (30 min), and following cardiac arrest (20 min). A representative rat (ID5513) is shown in *Top* and *Middle*, and averaged values for nine rats are shown in *Bottom*. Time is relative to the moment of cardiac arrest (CA; $T = 0$ s), and the time of ketamine/xylazine administration was marked as A on top of the graph. (*Middle*) EEG power around the time of cardiac arrest is displayed in an expanded scale, which shows 8 s of anesthetized state and 32 s of cardiac arrest. The time of cardiac arrest induction, defined as $T = 0$ s, is marked as a red dashed line. The z axis of spectrograms (*Top* and *Middle*) uses a log scale with blue indicating low power and red denoting high power. Three distinct stages of EEG power were detected following cardiac arrest: CAS1, CAS2, and CAS3. The absolute power of eight frequency bands from nine rats was compared during waking, anesthesia, and CAS3 states (*Bottom*). During waking and anesthesia, the mean and SD of power were calculated with 10-min EEG epochs, and taken from the middle of both (waking and anesthesia) 30-min periods. CAS3 values were derived from the peak powers (2-s bin). A significant ($P < 0.01$) increase of power was detected for low-gamma bands (γ_1 ; 25–55 Hz) over waking and anesthesia states, whereas power of other gamma bands, including medium gamma (γ_2 ; 65–115 Hz), high gamma (γ_3 ; 125–145 Hz), and ultra gamma (γ_4 ; 165–250 Hz), all diminished. Note that the 60-Hz notch and its superharmonics were excluded from the defined bandwidths. Significant increases ($P < 0.05$) in lower-frequency bands (<25 Hz), including delta (0.1–5 Hz), theta (5–10 Hz), alpha (10–15 Hz), and beta (15–25 Hz), were detectable following anesthesia compared with the waking state. (B) Analogous to A, except with a display of relative power averaged over the six EEG channels during waking (30 min), anesthesia (30 min), and following cardiac arrest (20 min). Because lower-frequency bands decrease in power following cardiac arrest, gamma bands became more dominant. All gamma bands showed significant ($P < 0.05$) increases in relative power following cardiac arrest compared with waking and anesthesia states, whereas the theta band showed a significant increase over the anesthesia state ($P < 0.05$) to a level indistinguishable with the waking state (*Bottom*). Of the analyzed frequency bands, the low-gamma bands showed a dramatic increase in relative power at near-death compared with both the waking state and the anesthetized state ($P < 0.0005$). Error bar denotes SD (* $P < 0.05$, ** $P < 0.01$, *** $P < 0.001$). The vertical axis on the right side of *Bottom* panels applies only to the gamma bands within the gray shaded areas. These results are not caused by pain associated with the cardiac arrest procedures, because comparable gamma surge was stimulated at near-death by CO_2 inhalation in rats (Fig. S3).

in power during anesthesia compared with the waking period (Fig. 2). In clear contrast to the anesthetized state, cardiac arrest stimulated a marked increase in global coherence (Fig. 3A, Lower). Increased mean coherence was identified for specific frequency bands unique to each of the three cardiac arrest states: high gamma (130–140 Hz) during CAS1, both high (120–130 Hz) and medium (80–100 Hz) gamma during CAS2, and all frequency bands for CAS3 (Fig. 3A, Lower). One striking distinction between CAS3 and the other states (waking, anesthesia, CAS1, CAS2), however, was

the markedly elevated coherence in low-gamma oscillations of 35–55 Hz that persisted for more than 15 s (Fig. 3A, Lower). The global coherence of low-gamma waves at near-death exhibited a more than twofold increase during CAS3 relative to waking ($P < 0.001$) and anesthetized ($P < 0.001$) states (Fig. 3B). In fact, low-gamma coherence in CAS3 exceeded coherence of all other bands and any time during the experiment. Theta oscillations during CAS3 also exhibited increased mean coherence compared with anesthesia ($P < 0.05$) and waking states ($P < 0.05$). The increased

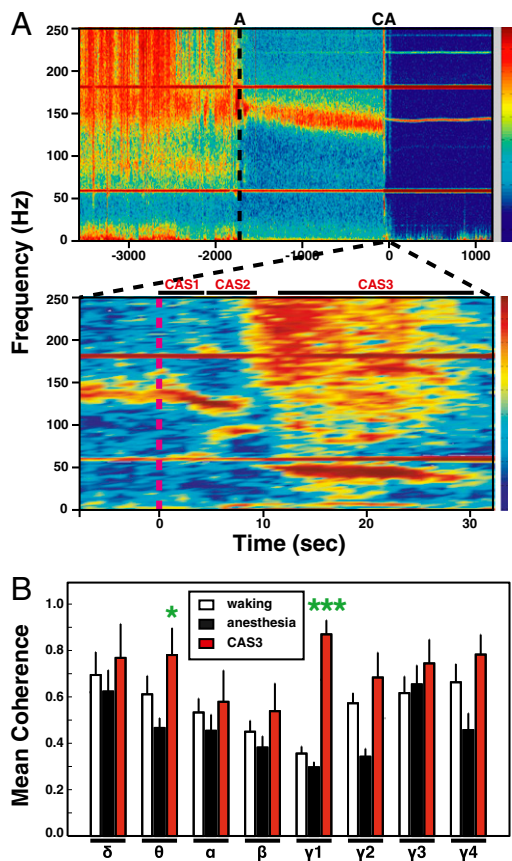


Fig. 3. Gamma coherence is markedly elevated after cardiac arrest. (A) Mean coherence values over six EEG channels during waking (30 min), anesthesia (30 min), and following cardiac arrest (20 min) are shown for one representative rat (ID5513). A narrow window of sharply increased coherence occurs across all frequency bands and is clearly detectable immediately following cardiac arrest (Upper); an expanded analysis is shown in Lower. Three distinct cardiac arrest states were detected: CAS1, CAS2, and CAS3. The z axis indicates the degree of coherence, with blue indicating low levels, and red indicating high levels, of coherence. Intense bands at both 60 and 180 Hz, and additional faint bands above 200-Hz ranges, are generated by ambient electromagnetic noise and persist for over 18 h after arrest. A 140-Hz band of uncertain significance appears to exhibit slight variation of frequency values during cardiac arrest. (B) The mean and SD of EEG coherence from six different locations were computed for eight indicated frequency bands during three states ($n = 9$). Significant ($P < 0.01$) increases in coherence of several frequency bands were found during CAS3 compared with anesthetized state: theta, γ_1 , γ_2 , and γ_4 ; of these, low-gamma (γ_1) oscillations displayed a significant ($P < 0.001$) increase in coherence compared with the waking state; theta coherence also showed a significant ($P < 0.05$) increase during CAS3 compared with the waking period. Error bar denotes SD (* $P < 0.05$, *** $P < 0.001$). These results are not a consequence of pain associated with the cardiac arrest procedures, because a nearly identical surge of gamma coherence was stimulated at near-death by CO_2 inhalation in rats (Fig. S4).

coherence does not result uniquely from cardiac arrest, because CO_2 inhalation induced a similar surge of global coherence at near-death (Fig. S4). Our results clearly indicate that mammalian brain activities become transiently and highly synchronized at near-death.

Anterior–Posterior Connectivity of Theta and Low-Gamma Waves at Near-Death Exceed the Waking State in Both Forward and Backward Directions. Presence of conscious brain activity has been associated with feedback connectivity, reflecting causal information transfer (22, 24). Feedback (frontal to parietal/occipital areas) and feedforward (occipital/parietal to frontal areas) connectivity analyses were applied to six frequency bands in consecutive 10-s bins (Fig.

4). Compared with the waking state, feedback and feedforward connectivity during anesthesia decreased in the delta, theta, alpha, beta, and medium-gamma (γ_2) bands as expected, whereas low-gamma (γ_1) showed no clear change (Fig. 4A). Following cardiac arrest, there was a transient rise of both feedback and feedforward connectivity for theta, alpha, beta, low-gamma (γ_1), and medium-gamma (γ_2) waves, which lasted for 30 s for gamma bands and 60 s for other bands (Fig. 4A). Of these bands, the low-gamma oscillations displayed the most striking elevation of connectivity in both directions with feedback dominance within the first 30 s of cardiac arrest (Fig. 4A). The levels of connectivity for all rats at near-death were nearly as high as waking for all frequency bands (except the delta bands) and significantly higher than anesthesia (Fig. 4B). Of the oscillatory signals analyzed, low-gamma waves exhibited the highest directed connectivity levels at near-death: fivefold higher in the feedforward ($P < 0.0001$) direction and eightfold higher in the feedback ($P < 0.0001$) direction compared with the waking state (Fig. 4B). This analysis also uncovered a marked directional asymmetry for the global connectivity of low-gamma oscillations at near-death: feedback (or top-down) connectivity was significantly ($P < 0.001$) higher than the feedforward connectivity. In addition to the significant changes in low-gamma oscillations, theta waves exhibited a twofold increase in both feedback ($P < 0.001$) and feedforward ($P < 0.001$) directions in the near-death state compared with the waking state (Fig. 4B). Thus, cardiac arrest induces a level of cortical directed connectivity in the near-death brain that far exceeds that observed during the waking state.

Low-Gamma Oscillations Are Coupled to Theta and Alpha Waves Following Cardiac Arrest. Cross-frequency coupling between phases of low-frequency waves and amplitudes of high-frequency bands has been shown to play a functional role in cognitive activities (34). Hence, we analyzed the effect of cardiac arrest on the coupling between the phase of delta, theta, and alpha bands, and the amplitude of all gamma bands (γ_1 – γ_4). As shown in Fig. 5, prominent coupling between the phase of theta waves and amplitude of medium gamma (γ_2) bands was found during the waking state (Fig. 5, Left). During anesthesia, the dominant coupling occurred between delta and high-gamma (γ_3) waves (Fig. 5, Center). Following cardiac arrest, two distinct and nonoverlapping clusters of coupling were identified during CAS3. The first occurred between theta (7–9 Hz) phase and low-gamma (30–40 Hz) amplitude, and the second was detected between alpha (10–15 Hz) phase and upper low-gamma (42–56 Hz) amplitude (Fig. 5, Right).

Comparison of CAS3 to waking and anesthesia revealed multiple state-dependent features of cross-frequency coupling. First, during waking and CAS3 (but not anesthesia), theta phase was strongly coupled to gamma amplitude. Second, the frequency range of coupled gamma amplitudes displayed state-specific changes: medium gamma (γ_2) during waking state, high gamma (γ_3) during anesthesia, and low gamma (γ_1) during CAS3. Last, CAS3 exhibited a distinct coupling between alpha phase and the upper low-gamma amplitude (42–56 Hz). Alpha–gamma coupling is associated with visual tasks in human (35) and is thought to play a role in perception of visual stimuli in humans during wakefulness (36). In monkey visual cortex, amplitude of gamma oscillations shows coupling with phases of both theta and alpha activity (7–14 Hz) (37). These past studies indicate that, in addition to theta–gamma coupling, alpha–gamma coupling is particularly important for visual perception. The high levels of global alpha–gamma coupling found in our studies suggest that the visual cortex may be highly activated during cardiac arrest.

Discussion

These data demonstrate that cardiac arrest stimulates a transient and global surge of synchronized gamma oscillations, which display

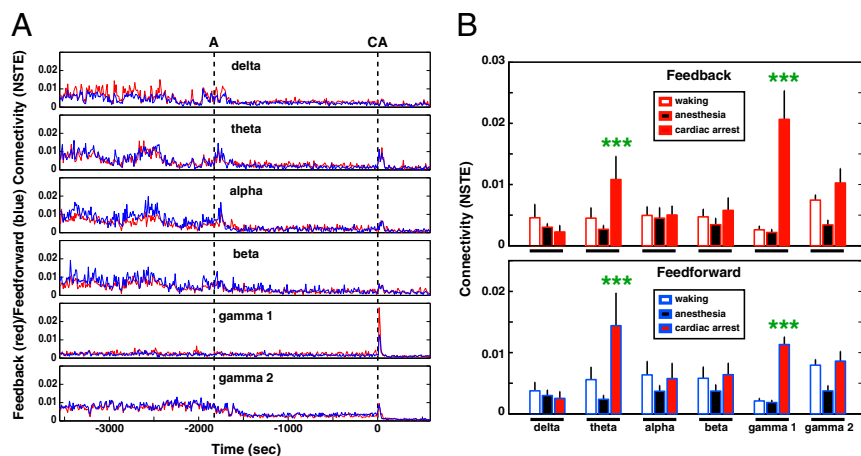


Fig. 4. Corticocortical connectivity surges following cardiac arrest. (A) Time course of feedback (red lines) and feedforward (blue lines) connectivity for the indicated frequency bands during waking (30 min), anesthesia (30 min), and following cardiac arrest (10 min). Connectivity between frontal and posterior (parietal and occipital areas) EEG activity was measured in 10-s bins by normalized symbolic transfer entropy (NSTE), a technique based in information theory. The vertical dashed lines denote the onset of anesthesia (A) and cardiac arrest (CA) induction. (B) The average feedback (Upper) and feedforward (Lower) connectivity at six frequency bands during waking, anesthesia, and following cardiac arrest in rats ($n = 9$). Connectivity index for both theta and gamma waves showed marked increase ($P < 0.001$) following cardiac arrest compared with both the waking and anesthesia states. Error bar denotes SD ($***P < 0.001$).

high levels of interregional coherence and feedback connectivity as well as cross-frequency coupling with both theta and alpha waves. Each of these properties of gamma oscillations indicates a highly aroused brain, and collectively, the data suggest that the mammalian brain has the potential for high levels of internal information processing during clinical death. The neural correlates of conscious brain activity identified in this investigation strongly parallel characteristics of human conscious information processing. Predictably, these correlates decreased during general anesthesia. The return of these neural correlates of conscious brain activity after cardiac arrest at levels exceeding the waking state provides strong evidence for the potential of heightened cognitive processing in the near-death state. Though neurophysiology at the moment of cardiac arrest has not been systematically studied in human cardiac arrest survivors, surges of electroencephalographic activity (measured by bispectral index) have been reported in humans undergoing organ donation after cardiac death (38). The consistent finding of a high-frequency EEG surge reflecting organized neurophysiologic activity in nine of nine rats undergoing cardiac arrest should prompt further studies in humans. Importantly, the essential results of increased gamma power and coherence were

confirmed with an alternative mode of death. Use of these unique experimental paradigms will allow detailed mechanistic dissection of neurophysiology of the dying brain in animal models, which could provide guidance for research on NDE after cardiac arrest in humans.

NDE represents a biological paradox that challenges our understanding of the brain and has been advocated as evidence for life after death and for a noncorporeal basis of human consciousness (39–42), based on the unsupported belief that the brain cannot possibly be the source of highly vivid and lucid conscious experiences during clinical death (9, 12). By presenting evidence of highly organized brain activity and neurophysiologic features consistent with conscious processing at near-death, we now provide a scientific framework to begin to explain the highly lucid and realer-than-real mental experiences reported by near-death survivors.

Materials and Methods

Animals. In all studies, the outbred Wistar strain of both male and female rats from Harlan was acclimatized in our housing facility for at least 1 wk before surgical implantation of electrodes. Following electrode implantation, rats were allowed to recover for at least 1 wk before recording. The experimental procedures were approved by the University of Michigan Committee on Use

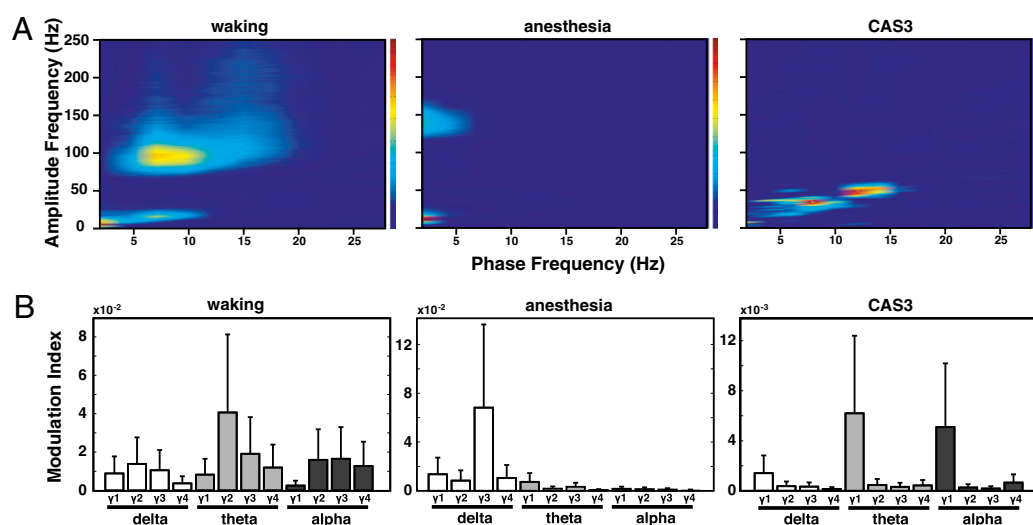


Fig. 5. Gamma power is modulated by theta and alpha phase in the near-death state. (A) Phase-amplitude comodulogram computed for EEG signals from waking (Left), anesthesia (Center), and following cardiac arrest at CAS3 (Right; $n = 9$). Phase-amplitude coupling was determined by computation of a MI (30), and only MI values significantly elevated above randomly shuffled surrogate data ($n = 50$ for each EEG data, $P < 0.05$; adjusted P values) were averaged over all six EEG channels of nine rats. (B) Mean MIs for phases of three slower waves [delta (0.5–5 Hz), theta (5–10 Hz), and alpha (10–15 Hz)] and amplitudes of four faster waves [γ_1 (25–55 Hz), γ_2 (65–115 Hz), γ_3 (125–175 Hz), and γ_4 (185–250 Hz)] computed for waking (Left), anesthesia (Center), and CAS3 (Right) states.

and Care of Animals. All experiments were conducted using adult rats (300–400 g). The rats were maintained on a light:dark cycle of 12:12 h (lights on at 6:00 AM) and provided with ad libitum food and water.

Electrode Implantation and Configuration. Rats were implanted with electrodes for EEG recordings under surgical anesthesia [1.8% (vol/vol) isoflurane]. The EEG signals were recorded through the screw electrodes implanted bilaterally on the frontal [anteroposterior (AP): +3.0 mm; mediolateral (ML): ±2.5 mm, bregma], parietal (AP: –3.0 mm; ML: ±2.5 mm, bregma), and occipital (AP: –8.0 mm; ML: ±2.5 mm, bregma) cortices. Electromyography (EMG) and electrocardiography (EKG) were recorded through flexible, insulated (except at the tip) multistranded wires (Cooner Wire) inserted into the dorsal nuchal muscle (EMG) and s.c. muscles flanking the heart (EKG). The EEG, EMG, and EKG electrodes were interfaced with two six-pin pedestals (Plastics One), and the entire assembly was secured on the skull using dental acrylic.

Signal Acquisition. Before the data collection, rats were acclimatized overnight in a recording chamber. Electrophysiological signals were recorded using Grass Model 15LT physiodata amplifier (15A54 Quad amplifiers) system (Astro-Med, Inc.) interfaced with a BIOPAC MP-150 data acquisition unit and AcqKnowledge (version 4.1.1) software (BIOPAC Systems, Inc.). The signals were filtered between 0.1 and 300 Hz and sampled at 1,000 Hz. EEG/EMG/EKG recording was initiated consistently at 10:00 AM to control for circadian factors. Baseline (waking consciousness) EEG signals were recorded for at least 30 min (up to 1 h). Recording was continued for 30 min under anesthesia induced by intramuscular injection of ketamine (25 mg/kg) and xylazine (25 mg/kg). At the end of this minimum 1 h of recording, cardiac arrest was

induced by intracardiac injection of potassium chloride solution (1 M, 0.5 mL). Recording was continued for an additional 30 min after cardiac arrest.

Signal Analysis Summary. The absolute power (Fig. 2A) was calculated based on discrete Fourier transformation for each 2-s-long EEG epoch with 1-s window overlapping and expressed in a log scale. The relative power (Fig. 2B) was calculated as the fraction of a specific frequency power in the total power over all frequency bands. For mean coherence of six EEG channels (Fig. 3), EEG was segmented into 2-s epoch with 1 s overlapping over all EEG recording. For each 2-s epoch, mean coherence was calculated based on magnitude squared coherence estimate using Welch's averaged periodogram method with 0.5-Hz frequency bin. The directed connectivity of EEG signals between frontal and posterior (parietal and occipital) brain regions (Fig. 4) was measured by normalized symbolic transfer entropy, which quantifies the causal relationship between two EEG signals in each direction. The modulation index (MI) was used to calculate phase-amplitude coupling (Fig. 5). For the waking and anesthesia periods, 10-min-long EEG signals (taken from the middle of the 30-min recording periods) were segmented into 10-s-long EEG epochs. For the CAS3 period, one 10-s epoch was selected from each of the six EEG channels. The MI between the phases of slower waves (0.5–30 Hz) and amplitudes of all measured oscillations (0.5–250 Hz) was calculated at each 10-s epoch for each rat at each EEG channel. Additional details about analysis can be found in [Supporting Information](#).

ACKNOWLEDGMENTS. We thank Bill Lipinski, Abhay Mathur, and Ramez Philips for technical assistance, and Duan Li for helpful comments on the manuscript. G.A.M. was supported by National Institutes of Health Grant GM098578 and the James S. McDonnell Foundation.

- Llinás R, Ribary U (1993) Coherent 40-Hz oscillation characterizes dream state in humans. *Proc Natl Acad Sci USA* 90(5):2078–2081.
- Strassman RJ, Qualls CR, Uhlenhuth EH, Kellner R (1994) Dose-response study of N, N-dimethyltryptamine in humans. II. Subjective effects and preliminary results of a new rating scale. *Arch Gen Psychiatry* 51(2):98–108.
- Griffiths RR, Richards WA, McCann U, Jesse R (2006) Psilocybin can occasion mystical-type experiences having substantial and sustained personal meaning and spiritual significance. *Psychopharmacology* 187(3):268–283; discussion 284–292.
- Lutz A, Greischar LL, Rawlings NB, Ricard M, Davidson RJ (2004) Long-term meditators self-induce high-amplitude gamma synchrony during mental practice. *Proc Natl Acad Sci USA* 101(46):16369–16373.
- Parnia S, Waller DG, Yeates R, Fenwick P (2001) A qualitative and quantitative study of the incidence, features and aetiology of near death experiences in cardiac arrest survivors. *Resuscitation* 48(2):149–156.
- van Lommel P, van Wees R, Meyers V, Elfferich I (2001) Near-death experience in survivors of cardiac arrest: a prospective study in the Netherlands. *Lancet* 358(9298):2039–2045.
- Greyson B (2003) Incidence and correlates of near-death experiences in a cardiac care unit. *Gen Hosp Psychiatry* 25(4):269–276.
- Moody RAJ (1975) *Life After Life* (Mockingbird Books, Seattle).
- van Lommel P (2011) Near-death experiences: The experience of the self as real and not as an illusion. *Ann N Y Acad Sci* 1234(1):19–28.
- Thonnard M, et al. (2013) Characteristics of near-death experiences memories as compared to real and imagined events memories. *PLoS ONE* 8(3):e57620.
- Mobbs D, Watt C (2011) There is nothing paranormal about near-death experiences: How neuroscience can explain seeing bright lights, meeting the dead, or being convinced you are one of them. *Trends Cogn Sci* 15(10):447–449.
- Facco E, Agrillo C (2012) Near-death experiences between science and prejudice. *Front Hum Neurosci*, 10.3389/fnhum.2012.00209.
- Greyson B, Holden JM, van Lommel P (2012) 'There is nothing paranormal about near-death experiences' revisited: Comment on Mobbs and Watt. *Trends Cogn Sci* 16(9), 445, author reply 446.
- Bearegard M, Paquette V (2008) EEG activity in Carmelite nuns during a mystical experience. *Neurosci Lett* 444(1):1–4.
- Cahn BR, Delorme A, Polich J (2010) Occipital gamma activation during Vipassana meditation. *Cogn Process* 11(1):39–56.
- Fries P (2009) Neuronal gamma-band synchronization as a fundamental process in cortical computation. *Annu Rev Neurosci* 32(1):209–224.
- Buzsáki G, Wang X-J (2012) Mechanisms of gamma oscillations. *Annu Rev Neurosci* 35(1):203–225.
- Sanders RD, Tononi G, Laureys S, Sleight JW (2012) Unresponsiveness ≠ unconsciousness. *Anesthesiology* 116(4):946–959.
- Rodriguez E, et al. (1999) Perception's shadow: Long-distance synchronization of human brain activity. *Nature* 397(6718):430–433.
- Dehaene S, Changeux J-P (2011) Experimental and theoretical approaches to conscious processing. *Neuron* 70(2):200–227.
- Tononi G (2012) Integrated information theory of consciousness: An updated account. *Arch Ital Biol* 150(2-3):56–90.
- Ro T, Breitmeyer B, Burton P, Singhal NS, Lane D (2003) Feedback contributions to visual awareness in human occipital cortex. *Curr Biol* 13(12):1038–1041.
- Imas OA, Ropella KM, Ward BD, Wood JD, Hudetz AG (2005) Volatile anesthetics disrupt frontal-posterior recurrent information transfer at gamma frequencies in rat. *Neurosci Lett* 387(3):145–150.
- Lee U, et al. (2009) The directionality and functional organization of frontoparietal connectivity during consciousness and anesthesia in humans. *Conscious Cogn* 18(4):1069–1078.
- Ku S-W, Lee U, Noh G-J, Jun I-G, Mashour GA (2011) Preferential inhibition of frontal-to-parietal feedback connectivity is a neurophysiologic correlate of general anesthesia in surgical patients. *PLoS ONE* 6(10):e25155.
- Boly M, et al. (2012) Connectivity changes underlying spectral EEG changes during propofol-induced loss of consciousness. *J Neurosci* 32(20):7082–7090.
- Benchenane K, et al. (2010) Coherent theta oscillations and reorganization of spike timing in the hippocampal-prefrontal network upon learning. *Neuron* 66(6):921–936.
- Molter C, O'Neill J, Yamaguchi Y, Hirase H, Leinekugel X (2012) Rhythmic modulation of θ oscillations supports encoding of spatial and behavioral information in the rat hippocampus. *Neuron* 75(5):889–903.
- Kahana MJ, Seelig D, Madsen JR (2001) Theta returns. *Curr Opin Neurobiol* 11(6):739–744.
- Siapas AG, Lubenov EV, Wilson MA (2005) Prefrontal phase locking to hippocampal theta oscillations. *Neuron* 46(1):141–151.
- Canolty RT, et al. (2006) High gamma power is phase-locked to theta oscillations in human neocortex. *Science* 313(5793):1626–1628.
- Jensen O, Colgin LL (2007) Cross-frequency coupling between neuronal oscillations. *Trends Cogn Sci* 11(7):267–269.
- Tort ABL, Komorowski RW, Manns JR, Kopell NJ, Eichenbaum H (2009) Theta-gamma coupling increases during the learning of item-context associations. *Proc Natl Acad Sci USA* 106(49):20942–20947.
- Canolty RT, Knight RT (2010) The functional role of cross-frequency coupling. *Trends Cogn Sci* 14(11):506–515.
- Voytek B, Canolty RT (2010) Shifts in gamma phase-amplitude coupling frequency from theta to alpha over posterior cortex during visual tasks. *Front Hum Neurosci*, 10.3389/fnhum.2010.00191.
- Siegel M, Donner TH, Engel AK (2012) Spectral fingerprints of large-scale neuronal interactions. *Nat Rev Neurosci* 13(2):121–134.
- Spaak E, Bonnefond M, Maier A, Leopold DA, Jensen O (2012) Layer-specific entrainment of gamma-band neural activity by the alpha rhythm in monkey visual cortex. *Curr Biol* 22(24):2313–2318.
- Auyong DB, et al. (2010) Processed electroencephalogram during donation after cardiac death. *Anesth Analg* 110(5):1428–1432.
- Chopra D (2006) *Life After Death: The Burden of Proof* (Harmony, New York).
- Long J, Perry P (2010) *Evidence of the Afterlife: The Science of Near-Death Experiences* (HarperOne, New York).
- van Lommel P (2010) *Consciousness Beyond Life: The Science of the Near-Death Experience* (HarperOne, New York).
- Alexander E (2012) *Proof of Heaven* (Simon & Schuster, New York).